

doi:10.15199/48.2025.02.22

## Comparison of elastic drive shaft models

**Abstract.** As part of this work, a computer simulation of the operation of an electromechanical system consisting of an electric motor coupled to a working machine via an elastic drive shaft was carried out. The simulation tests conducted and the test results obtained made it possible to compare the dynamics of the abovementioned electromechanical system represented by the same model of an electric motor and different models of the working mechanism, consisting of an elastic drive shaft and a load torque setter. In the simulation tests, the following models were considered for the elastic drive shaft: a distributed-parameter model based on the transmission line equations and lumped-parameter models, including multi-mass and two-mass models.

**Streszczenie.** W ramach tej pracy przeprowadzono komputerową symulację działania układu elektromechanicznego składającego się z silnika elektrycznego sprzężonego z maszyną roboczą za pośrednictwem sprężystego wału napędowego. Przeprowadzone badania symulacyjne i uzyskane wyniki badań pozwoliły na porównanie dynamiki ww. układu elektromechanicznego reprezentowanego przez ten sam model silnika elektrycznego i różne modele mechanizmu roboczego, składającego się ze sprężystego wału napędowego i zadajnika momentu obciążenia. W badaniach symulacyjnych uwzględniono następujące modele sprężystego wału napędowego: model o rozłożonych parametrach oparty na równaniach linii przesyłowej oraz modele o parametrach skupionych, w tym modele wielomasowe i dwumasowe. **(Porównanie modeli sprężystego wału napędowego)**

**Keywords:** electromechanical systems, elastic drive shafts, BLDC motor, modelling and simulation.

**Słowa kluczowe:** systemy elektromechaniczne, sprężyste wały napędowe, silnik BLDC, modelowanie i symulacja.

### Introduction

Electric drives are used in all industries and are the dominant consumer of electric energy. For this reason, the failure-free operation of these systems is essential. Analysis of the operating states of drive systems is often related to ensuring their operational safety. The key issue is to detect the occurrence of resonance and resonance-like phenomena as the most dangerous for the system. Dangerous phenomena also include significant-amplitude vibrations occurring in drive systems, especially in their working mechanisms, which are caused by sudden changes in driving torque. In such operating conditions, failures of mechanical components most often occur. Failure to take the abovementioned phenomena into account may lead not only to damage to the electric drives themselves, but sometimes to the suspension of production in the entire plant. Therefore, comprehensive research is needed to analyze the operating states of electrical and electromechanical systems. To achieve such a goal, it is necessary to conduct complex research, which is long-lasting and very expensive. The alternative is the analysis of the tested system represented in the form of a mathematical model. A mathematical model describes a physical object with a system of differential or algebraic equations or a combination of them.

Electric motors, which are part of electric drives, are coupled to working machines via drive shafts. Depending on the length and cross-section, drive shafts may have different susceptibility to moment of torsion, which determines the size of the angle of twist [1]. In the case of a short drive shaft, the size of the angle of twist is insignificant and can be neglected by assuming a rigid mechanical connection, while in the case of a longer drive shaft, the size of the angle of twist cannot be neglected and such connection should be considered elastic. Distributed-parameter models and lumped-parameter models are used to mathematically describe elastic drive shafts. The first group includes wave models [2], models based on the formal analogy between the drive shaft and the electric transmission line [3] and models based on the calculus of variations [4]. The second group includes two-mass models – with masses concentrated on both sides of the shaft [5] and multi-mass models, i.e. models with discretely distributed masses concentrated along the shaft axis [1]. Distributed-parameter models are constructed from partial differential equations that can be

solved analytically, but this is both tedious and time-consuming. An alternative is to use the method of lines (MOL), which involves: spatial discretization of a given equation (usually using the finite difference method), which leads to a system of ordinary differential equations, and then integration of the obtained equations with respect to time using numerical methods [1].

The electric transmission line equations based distributed-parameter drive shaft model [3], with the masses of the drive motor's rotor and the moving part of the working machine both attached to the ends of the shaft, is sometimes confused with the model of a two-mass structure [6,7]. Meanwhile, there is a fundamental difference between these models, which is related to the omission of the shaft mass in the two-mass structure. In this case, the omitted shaft mass is usually divided into two equal parts, which are attached to both ends of the shaft as lumped masses. Unlike a two-mass structure, in a distributed-parameter structure, the shaft mass is distributed linearly along the shaft axis and is continuous. Therefore, in a distributed-parameter structure, wave phenomena may occur when transmitting mechanical power along the shaft, and the reaction to the appearance of torque on one side of the shaft occurs with a delay on its other side, i.e. a certain time after the appearance of torque. In a two-mass structure, a similar reaction is immediate due to the omission of the shaft mass, i.e. a torque of the same value but with the opposite direction appears on both sides of the shaft at the same time. For this reason, wave phenomena do not occur in the two-mass structure. Based on the known shaft length, it is possible to estimate the frequency of the forced vibration of the torque, or torque component, applied to the beginning or end of the distributed-parameter drive shaft, at which wave phenomena will begin to play an important role:  $f = v/4l$ . Assuming  $l = 0.66$  m and the speed of mechanical wave propagation along the steel shaft  $v = 3102$  m/s, corresponding to a mass density of  $7850$  kg/m<sup>3</sup> and a shear modulus of  $80$  GPa,  $f = 1209$  Hz is obtained.

In this study, a simulation of the operation of an electromechanical system consisting of a brushless direct current (BLDC) motor coupled to a working machine via an elastic drive shaft was performed, with the role of the working machine being played by a load torque setter at the end of the shaft at the point of attachment of the working

machine's moving part. Two cases of the abovementioned moving part were considered: inertial moving part, i.e. with an additional rotating mass attached to the end of the drive shaft, and non-inertial moving part, i.e. without additional mass attached. The simulation tests carried out and the results obtained made it possible to compare the dynamics of the abovementioned electromechanical system represented by the same model of an electric motor and different models of the working mechanism consisting of an elastic drive shaft and a load torque setter. In the simulation tests, the following models were considered for the elastic drive shaft: a distributed-parameter model based on the transmission line's equations and lumped-parameter models – multi-mass and dual-mass.

### Models of elastic drive shafts

#### Two-mass, lumped-parameter model

Representing real mechanical systems with continuous mass distribution using models of lumped parameters based kinematic structures causes discrepancies in the analysis results compared to accurate models, but significantly simplifies the analysis. Additionally, these discrepancies decrease as the number of lumped parameters in the model increases. Representing the drive system containing an elastic element using a model with two lumped masses (two-mass system – Fig. 1) allows for maximum simplification of the model, but it cannot be used in all cases. Such a mathematical description works best in the case of mechanical systems in which the electric motor's rotor is coupled to the moving part of the working machine via a long shaft with a negligible moment of inertia, as opposed to significant moments of inertia of the mentioned elements of the mechanical system.

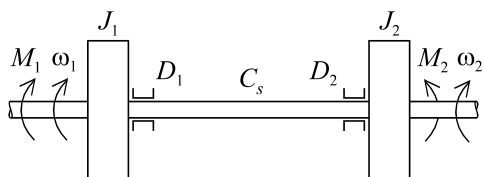


Fig. 1. Kinematic structure of a two-mass system (two lumped masses coupled via a long shaft with a negligible moment of inertia)

The equations for the considered structure are as follows:

$$\begin{aligned} \frac{d}{dt} L_1 &= M_1 - D_1 \omega_1 - D_{12}(\omega_1 - \omega_2) - M_c \\ \frac{d}{dt} L_2 &= M_c + D_{12}(\omega_1 - \omega_2) - D_2 \omega_2 - M_2 \\ \frac{d}{dt} \varphi &= \omega_1 - \omega_2 \end{aligned} \quad (1)$$

where  $M_1, M_2$  are the external torques applied to both sides of the shaft, in particular, the driving torque from the motor and the load torque from the working machine,  $\omega_1, \omega_2$  are the angular velocities at the points of application of external torques to the shaft,  $L_1, L_2$  are angular momentums, with  $L_1 = J_1 \omega_1, L_2 = J_2 \omega_2$ , from which  $\omega_1$  and  $\omega_2$  should be calculated and substituted into equations (1),  $J_1, J_2$  are the moments of inertia defined for the rotor of the drive motor and the moving part of the working machine,  $D_1, D_2$  are the coefficients of mechanical friction defined for the bearings,  $D_{12}$  is the coefficient of viscous friction inside the shaft,  $\varphi$  is the angle of shaft twist,  $M_c$  is the moment of shaft torsion, with  $M_c = C_s \varphi$ , which must also be substituted into equations (1),  $C_s$  is the torsional-elasticity coefficient. The form of equations (1) allows in the simplest way to take into

account the possible changes in moments of inertia as a function of angular velocity or angular position, as well as the changes in the torsional elasticity coefficient as a function of the angle of shaft twist.

#### Multi-mass, lumped-parameter model

The kinematic structure of the elastic drive shaft, divided into  $m$  elements as a result of discretization, is depicted in Figure 2, where  $J_1, \dots, J_m, C_{s,12}, \dots, C_{s,m-1,m}, D_{12}, \dots, D_{m-1,m}$  are the moments of inertia, torsional elasticity coefficients and mechanical friction coefficients of respective elements of the divided drive shaft;  $D_1, D_m$  are the mechanical friction coefficients defined for the bearings.

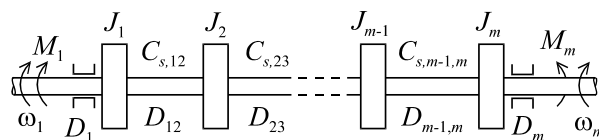


Fig. 2. Lumped parameter, multi-mass kinematic structure of elastic drive shaft

For the considered drive shaft,  $m$  equations of torques and moments of torsion, as well as  $m - 1$  equations of angles of twist can be written:

$$\begin{aligned} \frac{d}{dt} L_1 &= M_1 - D_1 \omega_1 - D_{12}(\omega_1 - \omega_2) - C_{s,12} \varphi_{12} \\ \frac{d}{dt} L_k &= C_{s,k-1,k} \varphi_{k-1,k} - \left. \begin{aligned} - D_{k-1,k}(\omega_{k-1} - \omega_k) - \\ - D_{k,k+1}(\omega_k - \omega_{k+1}) - \\ - C_{s,k,k+1} \varphi_{k,k+1} \end{aligned} \right\} \text{for } k = 2, \dots, m-1 \\ \frac{d}{dt} L_m &= C_{s,m-1,m} \varphi_{m-1,m} + D_{m-1,m}(\omega_{m-1} - \omega_m) - D_m \omega_m - M_m \\ \frac{d}{dt} \varphi_{k,k+1} &= \omega_k - \omega_{k+1} \quad \text{for } k = 1, \dots, m-1 \end{aligned} \quad (2)$$

#### Distributed-parameter model

In the article [3], the telegraphers' equations (3) with boundary conditions (4) and their solution (5), (6) defined by d'Alembert were proposed for the mathematical description of the drive shaft:

$$-\frac{\partial^2 M}{\partial x^2} = \frac{1}{v^2} \frac{\partial^2 M}{\partial t^2}, \quad -\frac{\partial^2 \omega}{\partial x^2} = \frac{1}{v^2} \frac{\partial^2 \omega}{\partial t^2}, \quad (3)$$

$$M_1(t) = M(x,t)|_{x=0}, \quad \frac{\partial M(0,t)}{\partial x} = \frac{\partial M(x,t)}{\partial x} \Big|_{x=0} \quad (4)$$

$$M_1(t) = z_v \omega_1(t) - z_v \omega_m(t - \frac{l}{v}) + M_m(t - \frac{l}{v}) \quad (5)$$

$$M_m(t) = -z_v \omega_m(t) + z_v \omega_1(t - \frac{l}{v}) + M_1(t - \frac{l}{v}) \quad (6)$$

where:  $v$  is the phase velocity given in m/s,  $v = 1/\sqrt{J' \cdot S'_c} = \sqrt{G/\rho}$ ,  $J'$ ,  $S'_c$  are the linear densities (density per unit length) of the moment of inertia and torsional susceptibility coefficient,  $S'_c = \rho/(GJ')$ ,  $\rho$  is the mass density given in kg/m<sup>3</sup>,  $G$  is the shear modulus given in GPa,  $M_1$ ,  $M_m$  are the moments of torsion at the beginning and end of the shaft, respectively,  $\omega_1$ ,  $\omega_m$  are the angular velocities at the beginning and end of the shaft,  $z_v$  is the wave impedance,  $z_v = \sqrt{J'/S'_c} = vJ'$ ,  $l$  is the shaft length. The abovementioned moments of torsion can also be presented in discrete form:

$$(7) \quad M_1(j) = z_v \omega_1(j) - z_v \omega_m(j-n) + M_m(j-n)$$

$$(8) \quad M_m(j) = -z_v \omega_m(j) + z_v \omega_1(j-n) + M_1(j-n)$$

with the predetermined initial conditions  $M_1(0)$ ,  $M_m(0)$ ,  $\omega_1(0)$  and  $\omega_m(0)$ , where:  $n$  is the number of modelling steps, this is a number that expresses the time of passage of the mechanical wave through the shaft,  $n = l/(vh)$ ,  $h$  is the width of the modelling step size,  $j = 0, 1, \dots$ . The time of passage of the mechanical wave through the shaft, corresponding to the number  $n$ , is given in equations (3) and (4) as  $l/v$ .

The angular velocities at the beginning and end of the shaft can be calculated from the equations of motion for the electric motor and the working machine:

$$(9) \quad \frac{d}{dt} L_e = M_e(t) - D_1 \omega_1 - D_{1m}(\omega_1 - \omega_m) - M_1$$

$$(10) \quad \frac{d}{dt} L_w = M_m - D_m \omega_m - D_{m1}(\omega_m - \omega_1) - M_w$$

where:  $M_e(t)$  and  $M_w(t)$  are the motor torque and the load torque from the working machine given in N·m,  $L_e = J_e \omega_1$ ,  $L_w = J_w \omega_m$ , from which  $\omega_1$  and  $\omega_m$  should be calculated and substituted into equations (9) and (10),  $J_e$  and  $J_w$  are the moments of rotor inertia for the electric motor and the working machine given in kg·m<sup>2</sup>,  $D_1$  and  $D_m$  are the coefficients of friction in the bearings. The terms  $D_{1m}(\omega_1 - \omega_m)$  and  $D_{m1}(\omega_m - \omega_1)$  with lumped parameters  $D_{1m}$  and  $D_{m1}$  have been introduced into equations (9) and (10) to take into account the viscous friction inside the shaft.

The drive shaft model based on the transmission line equations with the d'Alembert solution is an alternative to the multi-mass model based on ordinary differential equations as well as to the distributed parameter model based on partial differential equations. The advantage of the presented model is its simplicity, as it is based on discrete algebraic equations that do not require numerical integration, unlike models based on differential equations.

### Computer simulation results

The results of a computer simulation of the operation of an electromechanical system consisting of a 4 kW BLDC motor, an elastic drive shaft and a mass of  $J_m = 0.167$  kgm<sup>2</sup> attached to the end of the drive shaft are shown in Figures 3 to 6. The moment of inertia of the electric motor's rotor was assumed to be  $J_e = 0.025$  kgm<sup>2</sup>. The parameters of the steel drive shaft are as follows: length 0.66 m, diameter 0.02 m, mass density 7850 kg/m<sup>3</sup>, shear modulus  $G = 80$  GPa.

In the case under consideration, setting the rotational speed of the BLDC motor is performed by changing the

supply voltage (changing the duty cycle of the pulses controlling the electronic commutation of the BLDC motor using the PWM method). The BLDC motor control system considered in the simulation studies is not equipped with closed speed and current (or torque) control loops. The result of the lack of a closed current (or torque) control loop are the torque ripples (see Figure 5). In the process of starting the electric motor by changing the supply voltage according to the time ramp, the frequency of these ripples increases. At instant approximately 0.22 s, this frequency reaches twice the value of the natural frequency of the working mechanism containing the elastic drive shaft, which results in the system being stimulated to vibrate (the increased amplitude of torsional moment oscillations can be observed in the Figure 5). Resonance and resonance-like phenomena occur.

In the case of a drive shaft to the ends of which the masses of the rotor of the electric motor and the moving part of the working machine with significant inertias compared to the shaft are attached, i.e.  $J_e \gg J_s$  and  $J_m \gg J_s$ , where  $J_s$  is the moment of shaft inertia, the time responses of the electromechanical system under consideration, i.e. the motor torque, rotational speed and moment of torsion are almost identical for each drive shaft model, which can be seen from Figures 3 to 5.

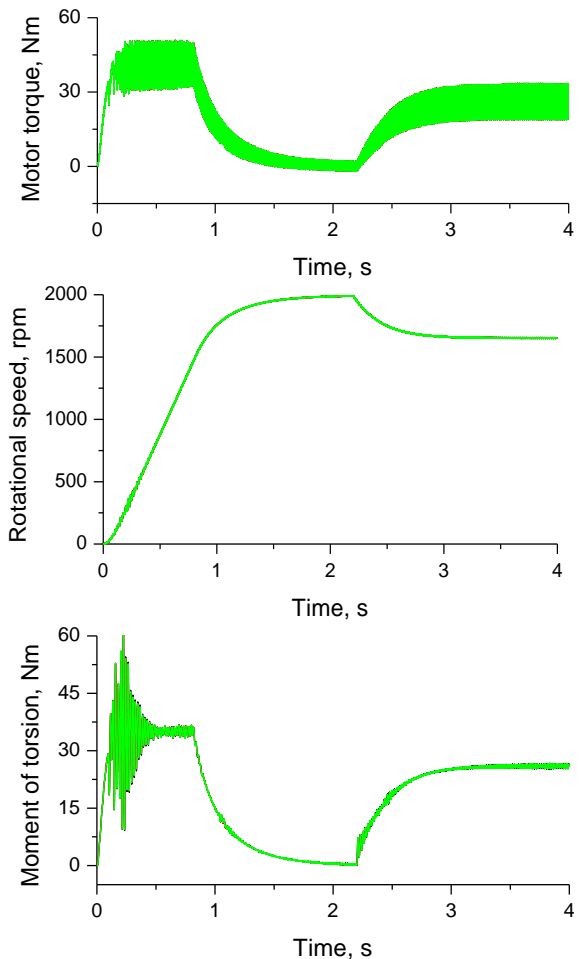


Fig. 3. Torque and rotational speed of the BLDC motor's rotor and moment of torsion at the beginning of the drive shaft during the start-up of the motor from the time  $t = 0$  s and during operation under the rated load (26 Nm) from the time  $t = 2.2$  s (time responses of all models overlap)

For the distributed-parameter model and the multi-mass model, there are differences in the moments of torsion at

the beginning and end of the shaft (Fig. 6) unlike the two-mass model. These differences are not significant compared to the rated motor torque (26 Nm). It is worth noting that the abovementioned differences are twice as large in the case of the distributed-parameter model.

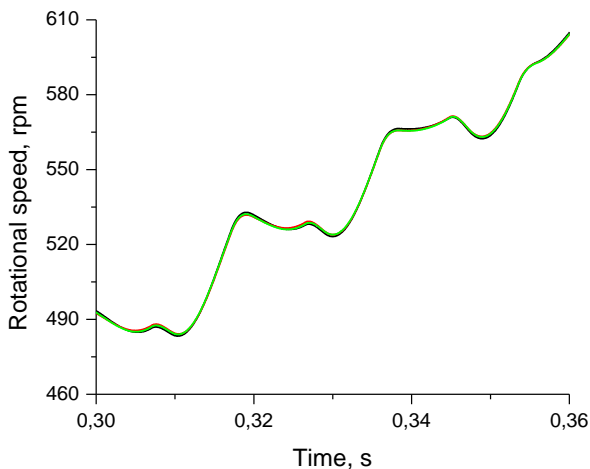


Fig. 4. Rotational speed of the motor in the time interval  $t = 0.3 \dots 0.36$  s; black line – distributed-parameter model, green line – multi-mass model, red line – dual-mass model

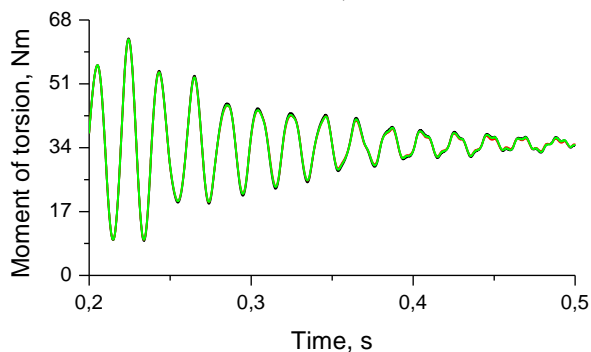
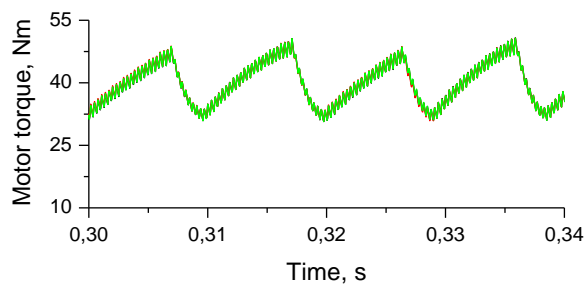


Fig. 5. Torque of the BLDC motor in the time interval  $t = 0.3 \dots 0.34$  s and moment of torsion at the beginning of the drive shaft in the time interval  $t = 0.2 \dots 0.5$  s

Also, very similar time responses, including motor torque and rotational speed (Fig. 7), can be observed for each drive shaft model in the absence of additional mass attached to the end of the shaft ( $J_m = 0$ ). The exception are changes in moments of torsion following a step (non-inertial) change in load at the end of the shaft (Fig. 8). In the case of a two-mass structure, at the shaft end the presence of a lumped mass equal to half of the omitted shaft mass was taken into account, in accordance with the rules for formulating a model of such a structure.

In the case of a distributed-parameter model, at the beginning of the shaft it can be observed a delayed reaction (black line in Figure 9) to a load torque step change at the end of the shaft (red line). This reaction can be observed

after approximately 0.2 milliseconds from the time in which the load torque step change occurred at  $t = 2.2$  s. This is the time (0.2 milliseconds) needed for the wave to travel from the end to the beginning of the shaft. This time can be calculated based on the length of the shaft and the speed of propagation of the mechanical wave inside the steel shaft. For the previously assumed values of the shaft length of 0.66 m and the speed of 3192 m/s, the calculated time is 0.207 ms.

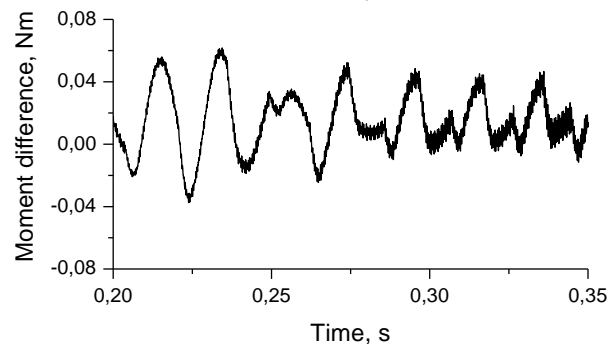
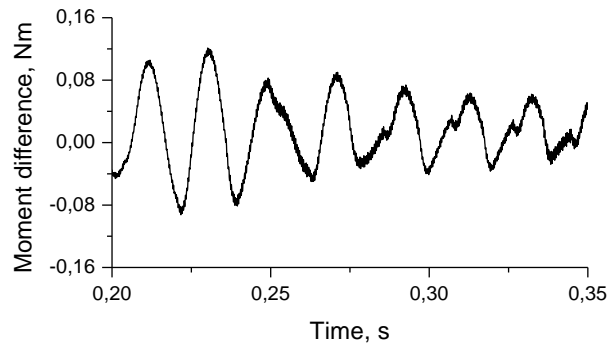


Fig. 6. Difference in moments of torsion at the beginning and end of the drive shaft, top – distributed-parameter model, bottom – multi-mass model

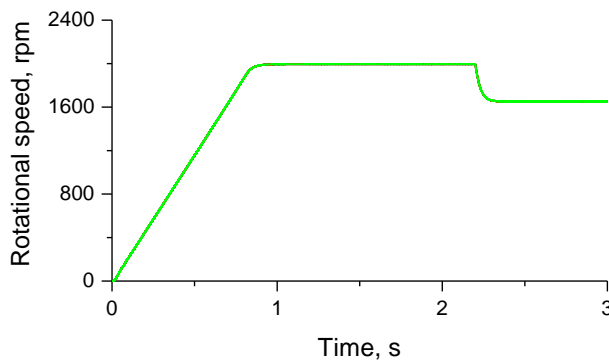
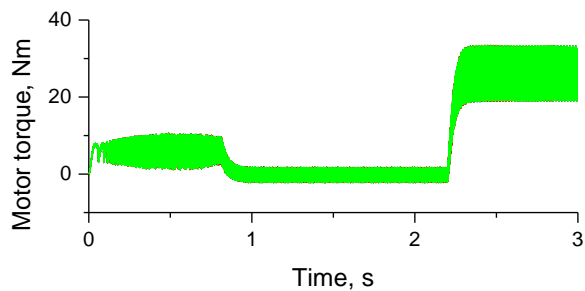


Fig. 7. Motor torque and rotational speed of the BLDC motor rotor during start-up from  $t = 0$  s and during operation under the rated load applied to the end of the drive shaft (26 Nm) from  $t = 2.2$  s (non-inertial load)

Similar phenomena can be observed in the case of the multi-mass model (Figure 10), which combines the features of a high-order inertial structure and an oscillatory structure. Meanwhile, the two-mass structure is only oscillatory in nature and does not undergo wave phenomena (Figure 8, red line). It is worth mentioning that in the case of a two-mass structure, the changes in the moment of torsion at the beginning of the shaft are the same as those at the end of the shaft. This results directly from the equations describing the two-mass structure (1): the same moments of torsion  $M_c$  are in both moment balance equations in (1).

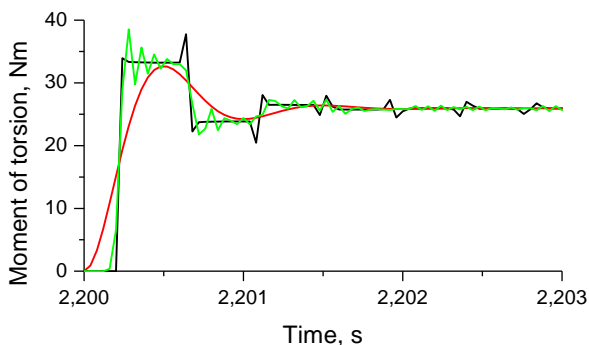


Fig. 8. Moments of torsion at the beginning of the drive shaft after applying a rated load of 26 Nm to the end of the shaft at  $t = 2.2$  s; black line – distributed-parameter model, green line – multi-mass model, red line – dual-mass model

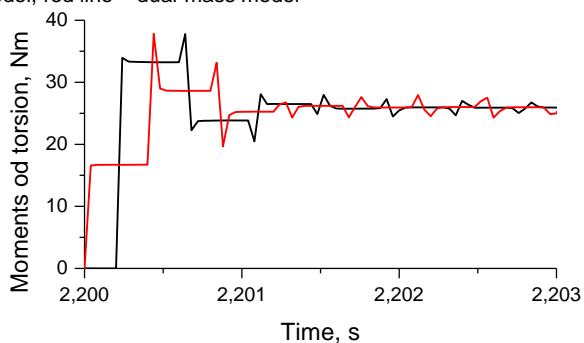


Fig. 9. Moments of torsion at the beginning (black line) and at the end (red line) of the drive shaft after applying a rated load of 26 Nm to the end of the shaft at  $t = 2.2$  s – distributed-parameter model

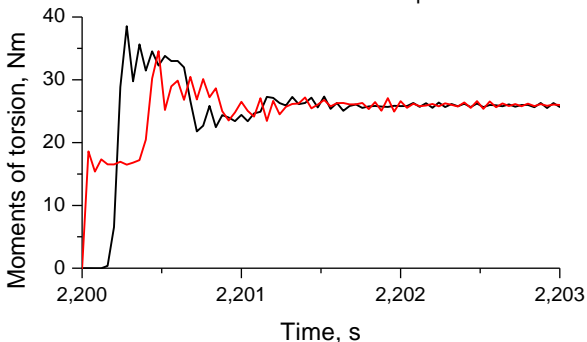


Fig. 10. Moments of torsion at the beginning (black line) and at the end (red line) of the drive shaft after applying a rated load of 26 Nm to the end of the shaft at  $t = 2.2$  s – multi-mass model

## Conclusions

Electromechanical systems consisting of electric drives, working machines and mechanisms containing long elastic drive shafts, are characterized by complex dynamics that are determined by all system components. Mathematical modelling of such systems involves formulating mathematical models for each component of the system and combining these models into a single whole. Particularly complex mathematical descriptions may appear in the case of elastic drive shafts, which cannot be described by the equations of a two-mass structure. In such a case, multi-mass models or distributed-parameter models can be used to mathematically describe the elastic drive shafts. These models can be used to analyze the influence of control and load on the electromechanical system, as well as emergency states related to the occurrence of resonant or resonant-like phenomena. The simulation results can be used to design electric drives, as well as to optimize the operation of electromechanical systems.

This article presents a comparative analysis of various models of elastic drive shaft. In the case of a distributed-parameter model, the reaction at the beginning of the shaft to a change in the load torque at the end of the shaft occurs a certain time after this change presence. This is the time required for the wave to travel from the end to the beginning of the shaft. Similar phenomena can be observed in the case of the multi-mass model. Meanwhile, the two-mass structure is oscillatory and does not undergo wave phenomena.

**Authors:** Andrzej Popena, PhD, D.Sc., Associate Prof.; Marjan Nowak, PhD, Czestochowa University of Technology, Faculty of Electrical Engineering, 17 Armii Krajowej av, 42-200 Czestochowa, E-mail: andrzej.popena@pcz.pl, marjan.nowak@pcz.pl

## REFERENCES

1. Popena A., Mathematical modelling of transmission shafts based on electrical and mechanical similarities, *Przegląd Elektrotechniczny*, 95 (2019), no. 12, 196-199
2. Swanson, D.C., Signal processing for intelligent sensor systems with MATLAB®, 2nd ed.; CRC Press, (2017), 7-23
3. Popena A., Szafraniec A., Chaban A., Dynamics of Electromechanical Systems Containing Long Elastic Couplings and Safety of Their Operation, *Energies*, 7882 (2021), no. 14, 1-18
4. Chaban A., Lis M., Szafraniec A., Jedynek R., Application of Genetic Algorithm Elements to Modelling of Rotation Processes in Motion Transmission Including a Long Shaft, *Energies*, 14 (2020), no. 1, 115
5. O'Sullivan T., Bingham C.C., Schofield N., High-performance control of dual-inertia servo-drive systems using low-cost integrated SAW torque transducers, *IEEE Trans. on Ind. Electron.*, 53 (2006), no. 4, 1226-1237
6. Kabziński J., Mosiołek P., Integrated, Multi-Approach, Adaptive Control of Two-Mass Drive with Nonlinear Damping and Stiffness, *Energies*, 5475 (2021), no. 14, 1-23
7. Gasiyarov V.R., Radionov A.A., Loginov B.M., Zinchenko M.A., Gasiyarova O.A., Karandaev A.S., Khrumshin V.R., Method for Defining Parameters of Electromechanical System Model as Part of Digital Twin of Rolling Mill, *J. Manuf. Mater. Process.*, 183 (2023), no.7, 1-20